

# Applications of paleomagnetism in the volcanic field: A case study of the Unzen Volcano, Japan

Hidefumi Tanaka<sup>1</sup>, Hideo Hoshizumi<sup>2</sup>, Yuki Iwasaki<sup>3</sup>, and Hidetoshi Shibuya<sup>3</sup>

<sup>1</sup>Kochi University, Dept. of Education, Kochi 780-8520, Japan

<sup>2</sup>Geological Survey of Japan, AIST, 1-1-1 Higashi, Tsukuba 305-8567, Japan

<sup>3</sup>Kumamoto University, Dept. of Earth Sciences, Kumamoto 860-8555, Japan

(Received December 4, 2003; Revised June 19, 2004; Accepted June 22, 2004)

A case study is presented for applications of paleomagnetism in the volcanic field. First, the importance of magnetic cleaning was demonstrated for the present-day pyroclastic flow. Some blocks contained a very large secondary component which was removed only after heating to temperatures over 400°C. Second, progressive thermal demagnetization was used to determine the cooling history of volcanic products. In the case of a block-and-ash flow found at a depth of 450 m in a drill core, the emplacement temperature varied from block to block, giving inconsistent results. Some blocks, however, might have undergone rotations during cooling because one or two sharp kinks were often recognized in the orthogonal plots of thermal demagnetization. In another case of a Holocene block-and-ash flow, the remanence directions for block samples were completely scattered. This contradictory observation is interpreted by an eruptive sequence that the blocks had already cooled down below the blocking temperature at the summit when the lava dome was at the stage of endogenous formation. Finally, case studies of lava identification by remanence directions are given. For some lava flows which are coeval in terms of volcano-stratigraphy, remanence directions are different beyond the error, suggesting a short time gap between their extrusion.

**Key words:** paleomagnetism, progressive thermal demagnetization, block-and-ash flow, exogenous dome, endogenous dome, Unzen Volcano.

## 1. Introduction

Most lava flows and welded tuffs have a remanence aligned to the ambient geomagnetic field at the time of their formation, which is called a thermoremanent magnetization (TRM). Non-welded pyroclastic flows have a TRM or a partial TRM according to how high the formation temperature was. This gives us an opportunity to estimate the emplacement temperature ( $T_E$ ) of pyroclastic flows. In the pioneering work of Aramaki and Akimoto (1957), bulk remanence of rock fragments, which is called a natural remanent magnetization (NRM), was measured. Such a method of measuring NRM directions allows us only to know whether the  $T_E$  of the pyroclastic deposit was higher or lower compared to the Curie temperature ( $T_C$ ) of the fragment; the temperature at which the intrinsic magnetism of the magnetic mineral disappears. Later studies used the method of progressive thermal demagnetization to confine  $T_E$  more accurately (Yamazaki *et al.*, 1973). Remanence of pyroclastic deposits is often contaminated by secondary components of viscous origin (viscous remanent magnetization; VRM) or chemical origin (chemical remanent magnetization; CRM). Hence, studies of  $T_E$  of pyroclastic flows need to involve careful analysis of the progressive thermal demagnetization (Kent *et al.*, 1981). In the case of hemoilmenite-bearing pumice fall,

further petromagnetic studies could reveal other information such as cooling rate (Ozima *et al.*, 2003).

The geomagnetic field fluctuates in direction and intensity, and the temporal variation of direction usually amounts to 2 to 8° per 100 years (Merrill *et al.*, 1996). Once a standard curve of the secular variation (SV) of the paleomagnetic field is established for a certain time interval, it can be used to estimate an age of a volcanic rock as long as it is known from other methods that this rock was formed during a specific time interval. This method has often been used in archeology (Eighmy and Sternberg, 1990), and can be equally applied to volcanic rocks for the last four or five thousand years (Holcomb *et al.*, 1986; Hagstrum and Champion, 1994). Combining with measurements of intensities of the paleomagnetic field (paleointensity) makes the method more powerful, as shown by Miki (1999) who successfully estimated ages of andesite lavas in the Sakurajima Volcano, Japan. Prior to the Holocene, it becomes difficult to establish the standard SV curve of the paleomagnetic field, giving a limit to the paleomagnetic dating of volcanic rocks. Nevertheless, remanence directions of volcanic rocks give a tool to identify whether there was a certain amount of time lag among their extrusion beyond the limit of radiometric dating method (Bogue and Coe, 1981; McIntosh, 1991). Relative dating based on a comparison of remanence directions has also been considered in archeomagnetism when a standard SV curve is not available (e.g., Downey and Tarling, 1984).

This study reports a case study of paleomagnetic applica-

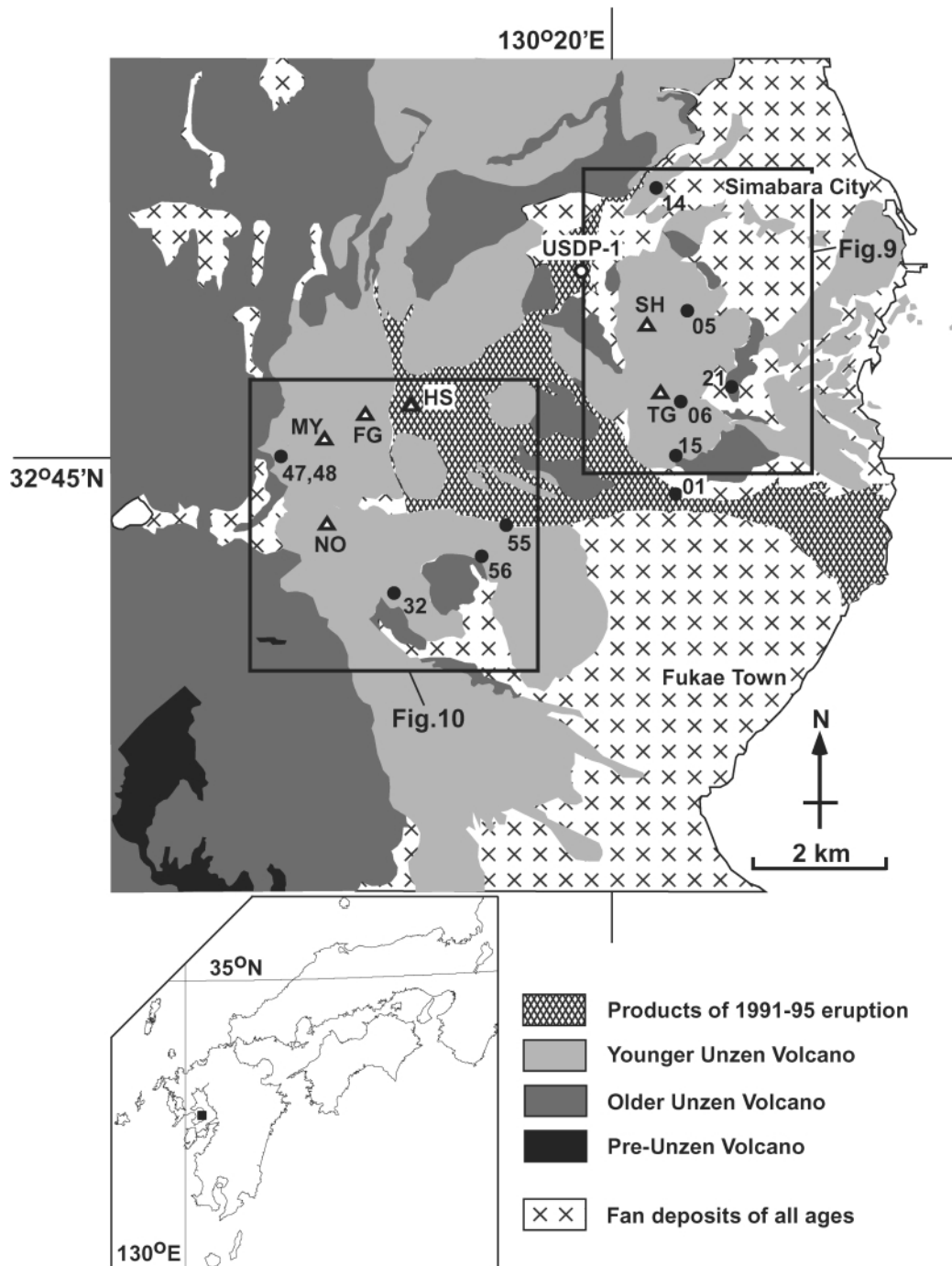


Fig. 1. Geological map of the Unzen Volcano which was simplified from Hoshizumi *et al.* (1999). Left bottom, inset is a map of southwestern Japan showing a solid rectangle indicates the area the geological map covers. Rectangle frames in the geological map indicate the areas covered by Figs. 9 and 10. An open circle indicates one of the drill sites (USDP-1) where paleomagnetic measurements were taken of one of block-and-ash flows. Circles indicate site locations of paleomagnetic samples which are all from the Younger Unzen. Triangles indicate the peaks of the volcanoes of the Younger Unzen, and their abbreviations are the followings. NO; Nodake (Nodake Volcano, 120–70 ka), MY; Myokendake (Myokendake Volcano, 40–27 ka), FG, HS; Fugendake and Heisei-Shinzan (Fugendake Volcano, 27–0 ka), SH, TG; Shichimenzan and Tenguyama (Mayuyama Volcano, 5–0 ka).

tions in the Unzen Volcano, Kyushu, southwestern Japan. In 1999, the Unzen Scientific Drilling Project (USDP) started as a multi-disciplinary study with drilling which also included various surface studies using geological and geophysical methods. As a part of the study of the eruptive history, paleomagnetic measurements were made mainly of some of the surface rocks. The contribution of paleomagnetism to

the study of the eruptive history of the volcano was not large, due to the fact that there is no standard SV curve of the paleomagnetic direction prior to the Holocene. However, some interesting results were obtained through paleomagnetic measurements. Some of the paleomagnetic applications will be presented in this study, and some useful suggestions will be discussed. Throughout the project, extensive work was car-

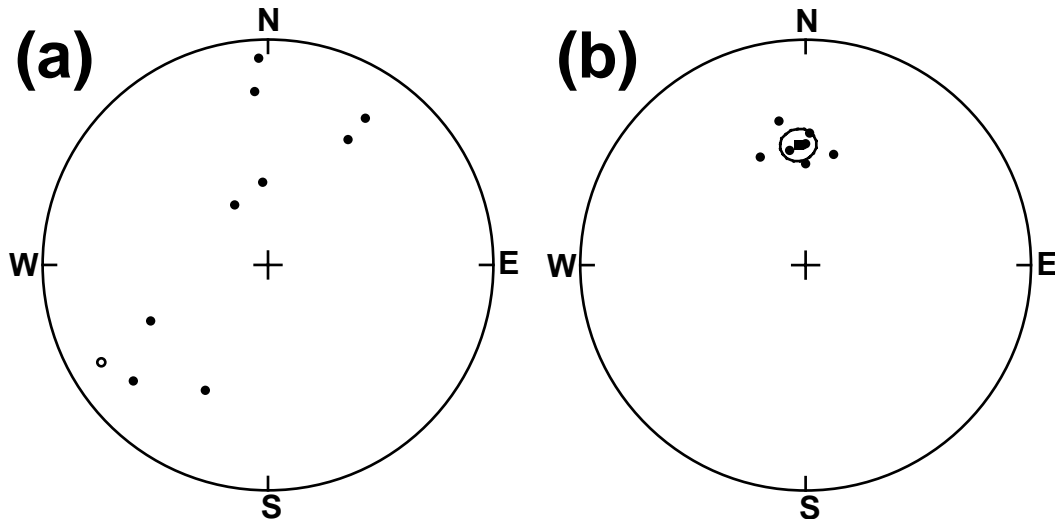


Fig. 2. Examples of extremely large secondary remanences contained in a present-day pyroclastic deposit which were finally removed by thermal demagnetization. Equal area plots of NRM directions and primary remanence directions are shown in (a) and (b), respectively. Closed and open circles indicate downward and upward directions, respectively, and a closed square in (b) is a mean remanence direction where the oval around it indicates a 95 percent confidence circle. The pyroclastic flow is a large-scale block-and-ash flow which was generated on 8 June 1991.

ried out for the usual study of paleosecular variation from volcanic rocks (e.g., Tanaka and Kobayashi, 2003), and this will be published elsewhere.

## 2. Geology and Sampling

The Unzen Volcano is a composite volcano with many lava domes, thick lava flows, and pyroclastic deposits of andesite to dacite composition. It is in the western part of Kyushu Island, southwest Japan. Being about 70 km to west of the volcanic front makes it quite distinct from other volcanoes in the Kyushu Island. It is located in the large-scale graben which traverses the central Kyushu, and is cut by normal faults at the northern and southern fronts. Estimated total subsidence within the graben amounts to  $\sim 1$  km since it started its volcanic activity about 0.5 My ago.

The eruptive history of the Unzen Volcano surveyed after the eruption of 1990–1995 (Watanabe and Hoshizumi, 1995; Hoshizumi *et al.*, 1999), was further developed by intensive studies of the USDP and other surficial studies (Hoshizumi *et al.*, 2002; Uto *et al.*, 2002). The composite volcanic edifice is subdivided into Older and Younger Unzen Volcanoes. The lower half of the Older Unzen (500–300 ka) is composed of dacite pumice flows with fall and lahar deposits. During this period, there were explosive pumice eruptions and lava effusions. The upper half of the Older Unzen (300–150 ka) is characterized by many pyroclastic flows and lahar deposits with a few andesitic to dacitic lava flows. Thick phreatomagmatic products, found from USDP cores, indicates extensive subsidence of the graben in this period. The Younger Unzen Volcano (150–0 ka) comprises of four volcanoes which are the present-day primary topographic features. In this period, volcanic activity moved east, and the lava domes and the pyroclastic flows became of a smaller scale compared to those in the Older Unzen.

Figure 1 shows a geological map of the Unzen Volcano

which was simplified from Hoshizumi *et al.* (1999). In the figure, triangles are the peaks of the volcanoes of the Younger Unzen. An open circle indicates one of the drill sites (USDP-1) in which paleomagnetic measurement was made to one of the block-and-ash flows. Circles indicate site locations of paleomagnetic samples which are all from the Younger Unzen, including the 1991 pyroclastic flow (UZ01), lava dome and pyroclastic flows of about 5 ka from the Mayuyama Volcano (UZ05, 06, 14, 15, 21), and  $\sim 100$  ka Fukkoshi Lava (UZ32, 47, 48, 55, 56). Rectangular frames in Fig. 1 indicate the areas covered by Figs. 9 and 10, showing the Mayuyama Volcano and the Fukkoshi Lava that were paleomagnetically studied.

Core samples of 25 mm in diameter were collected at each site by a portable drill. Orientation of the core was measured by a sun compass when the sun was available. Remanences were measured by a spinner magnetometer SMD-88 of Natsuhara Co. Progressive thermal demagnetization was performed on all samples from a pyroclastic flow. For lava flows, one pilot sample was used for each of the progressive AF and thermal demagnetizations. Blanket AF demagnetization with a single optimal step was used for the rest.

## 3. Emplacement Temperature of a Pyroclastic Flow

### 3.1 Case of extremely large secondary remanences

The remanence direction and  $T_E$  of the present-day pyroclastic flow was examined to ascertain the basic principle of the paleomagnetic method. This pyroclastic flow was generated as a block-and-ash flow on a large scale on 8 June 1991. Ten oriented samples were collected from five blocks by a portable drill. It was rather a surprise that the NRM directions were very scattered, as shown in Fig. 2(a). This is because the present-day volcanic rocks usually contain only small secondary remanences, even though they exist in al-

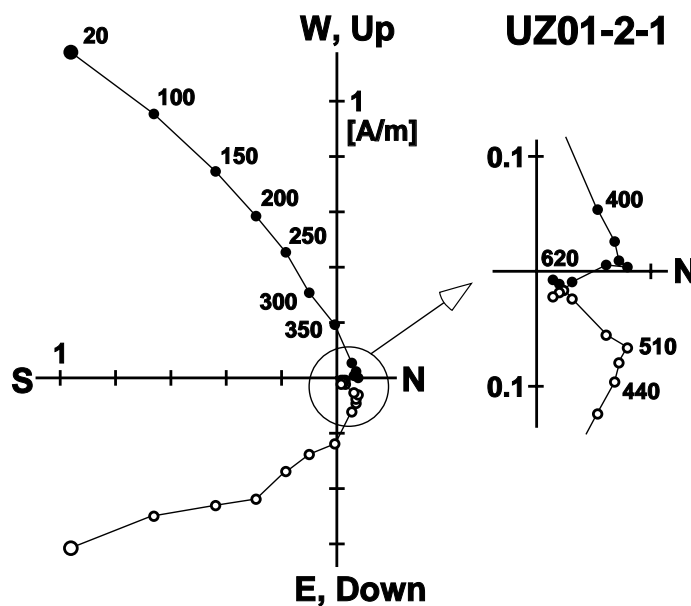


Fig. 3. An example of an orthogonal plot of thermal demagnetization for the present-day block-and-ash flow deposit whose sample directions are shown in Fig. 2. Closed and open circles indicate end points of the remanence projected on the horizontal and vertical planes, respectively. It is seen that a large secondary component was removed at 510°C.

most all cases. Hence, doubt was cast whether this pyroclastic flow was really hot in spite of actual observations on the day of generation. When progressive thermal demagnetization was made, however, it turned out that most samples contain a very large secondary magnetization. Figure 3 shows an orthogonal plot of UZ01-2-1 which contained the largest secondary component. When the progressive thermal demagnetization was applied, the secondary component was removed at 510°C and a remanence component of a reasonable direction finally appeared above this temperature, as shown in the enlarged plot in Fig. 3. The component of a remanence (RM) acquired under the ambient field during the formation of the rock is generally called a primary magnetization and is hereafter termed a primary RM. Primary RMs are well grouped, as shown in Fig. 2(b), and the mean remanence direction of ( $I=45.4^\circ$ ,  $D=-3.6^\circ$ ,  $\alpha_{95}=6.3^\circ$ ) is in good agreement with the present-day geomagnetic field of ( $I=46.5^\circ$ ,  $D=-6.1^\circ$ ) at the site calculated from DGRF1990 (Barton *et al.*, 1997).

The primary RM of the 1991 pyroclastic flow disappeared at  $T_C$  in the progressive demagnetization. This indicates that the  $T_E$  was equal to or higher than  $T_C$  because, otherwise, the primary RM should be demagnetized at a certain temperature, called a blocking temperature ( $T_B$ ), which is lower than  $T_C$ . Nevertheless, it is difficult to know the origin of the very large secondary component. One possible explanation would be isothermal remanent magnetization (IRM) induced by a lightning strike. Lightning-induced remanence is usually very strongly magnetized (Verrier and Rochette, 2002), but the remanences of the 1991 pyroclastic flow are not strong, suggesting another possibility of artificial disturbance such as the effect of construction vehicles. The result of the 1991 pyroclastic flow might be an extreme case but demonstrates that applying a progressive thermal demagnetization is important in the paleomagnetic measurements of

pyroclastic flows.

### 3.2 Post-placement block rotations within a flow

More than 10 block-and-ash flows were found from the vertical drill core (USDP-1) of 752 m length, which was drilled at the northeastern flank of the Unzen Volcano (Hoshizumi *et al.*, 2002). Eight blocks were collected from a typical block-and-ash flow found at 450 m depth, which was later dated as  $221 \pm 21$  ka (K-Ar method; Matsumoto *et al.*, 2002). Eight dense to slightly vesiculated blocks of a size of about 20 cm were found within the core of the pyroclastic flow which spans a thickness of about 8 m. A few cylindrical samples of 2.5 cm in diameter and 2.2 cm in length were drilled from each block for paleomagnetic measurements. Sample orientation was made only along the vertical line. Hence, the azimuth of the sample is arbitrary except for those from each of 1 m section of the drilled core in which a common reference was marked. However, even for the same 1 m section, the cores were often separated into several rods. Hence, the declination of the remanences was not taken into consideration.

Progressive thermal demagnetization was carried out on all samples. Three types of orthogonal plots were found. The first type reveals only one component of the remanence, as shown in Figs. 4(a) and (b). The second type shows two components, as shown in Figs. 4(c) and (d), though in the former the high temperature component occupies only a small part of the total remanence. In the third type, shown in Figs. 4(e) and (f), there are three components which are separated by sharp kinks.

It is obvious that those blocks which give the type 1 orthogonal plot were cooled from high temperature, indicating that  $T_E$  was higher than  $T_C$ . For the cases of type 2 and 3 orthogonal plots, the remanence component with the lowest  $T_B$  is the one which was acquired at the final stage of

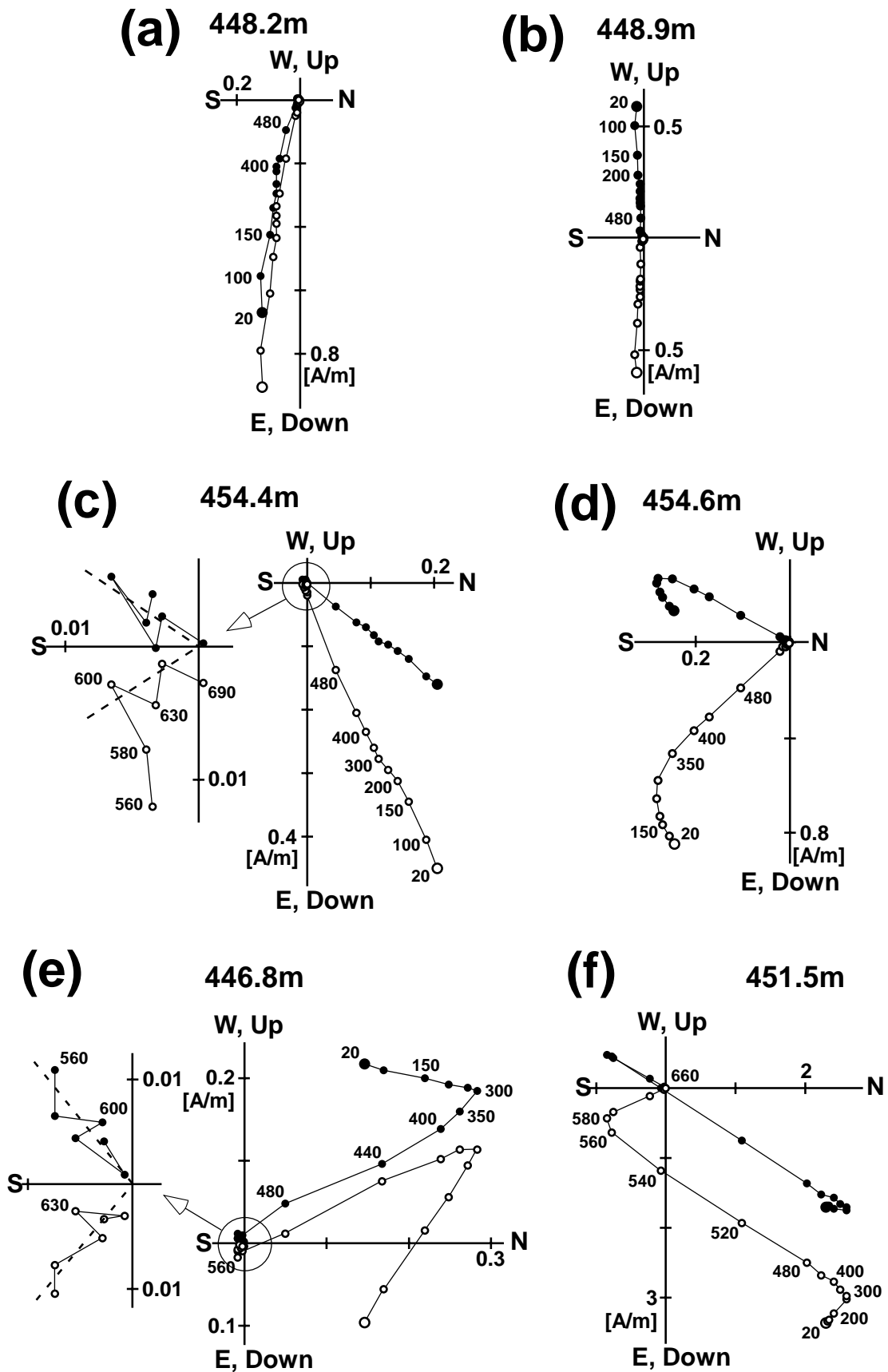


Fig. 4. Three types of orthogonal plots found from a block-and-ash flow at 450 m depth of a drilled core (USDPI-1); the first type with one component (a, b), the second type with two components (c, d), and the third type with three components which are separated by sharp kinks (e, f). Two very sharp kinks recognized in the third type indicate that these blocks suffered two rotations during cooling.

Table 1. Remanence components revealed by thermal demagnetization for eight blocks from a pyroclastic flow found at about 450 m depth of the drill core (USDP-1). Underlined is the possible primary remanence.

Depth (m)	High $T_B$ component		Middle $T_B$ component		Low $T_B$ component	
	Inc (°)	$T_B$ span (°C)	Inc (°)	$T_B$ span (°C)	Inc (°)	$T_B$ span (°C)
446.8	37.0	560–690	–22.0	300–540	<u>55.9</u>	<u>20–300</u>
448.2	<u>53.9</u>	<u>100–690</u>				
448.9	<u>46.0</u>	<u>100–690</u>				
450.6	<u>52.6</u>	<u>520–690</u>			–62.6	20–250
451.5	23.3	580–690	29.6	300–560	<u>49.4</u>	<u>20–250</u>
452.9	20.3	520–690			<u>49.2</u>	<u>20–350</u>
454.4	28.0	600–690	<u>58.7</u>	<u>20–560</u>		
454.6	<u>39.6</u>	<u>350–690</u>			48.2	20–150

Note: Inc; inclination,  $T_B$ ; blocking temperature.

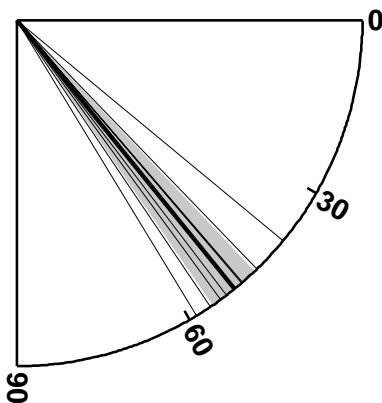


Fig. 5. Rose diagram of inclination-only data for the possible characteristic remanences obtained from the drilled core (Fig. 4). The thick line and the shaded sector indicate the mean inclination and 95 percent confidence angle determined by the method of Enkin and Watson (1996). Thin lines indicate the inclinations of each remanence direction. Consistent remanence directions is obvious in spite of different estimations of the emplacement temperature.

the cooling history. Two very sharp kinks at about 300 and 580°C, recognized in Figs. 4(e) and (f), indicate that these blocks suffered two rotations at these temperatures. An important point which we should pay attention to is the possibility of a VRM origin for the lowest  $T_B$  component, especially when the samples are prone to VRM acquisition (Saito *et al.*, 2003). Those lowest  $T_B$  components, shown in Figs. 4(e) and (f), are unlikely to be of VRM origin because of their sharp kinks in the orthogonal plots. However, we judged that the lowest  $T_B$  component recognized in Fig. 4(d) was actually of VRM origin because the remanence direction continuously changed.

All the remanence components for each block are summarized in Table 1 in which a possible primary RM is underlined. As those primary RMs are found from different ranges of temperature, the results might look very inconsis-

tent. However, the correctness of these remanence components as primary RMs is proved by consistent inclinations, as shown in the rose diagram (Fig. 5) in which thin lines indicate inclinations of each remanence direction. Statistics of inclination-only data were calculated by the method of Enkin and Watson (1996), giving a mean inclination of 51.0° and a 95 percent confidence angle of 4.5°, which are shown by a thick line and a shaded sector, respectively, in the figure. The mean inclination is quite reasonable as a typical value for a TRM acquired about 200 ka. Hence, inconsistent  $T_E$ s among the blocks are obvious. This could be interpreted as being due to blocks that came to rest at different temperatures. Hence, block-and-ash flows are not uniform in temperature. However, we favor another interpretation: that some of the blocks rotated within the flow, while others were not disturbed, although the initial emplacement temperature was high. A good indication of the block rotation during cooling is observed in the orthogonal plots shown in Figs. 4(e) and (f). The highest  $T_B$  component must be carried by hematite, which is in accordance with the reddish color of the blocks.

### 3.3 High temperature emplacement with scattered paleodirections

A cautionary case from two pyroclastic flows is illustrated here. It is highly likely from lithologic observations that both the 4 ka Mutsugi Pyroclastic Flow (UZ14) and the 5 ka Kita-Kamikoba Pyroclastic Flow (UZ15) are block-and-ash flows that erupted from the Mayuyama Volcano. The pyroclastic flow deposits are composed of dacite dense blocks set in finer materials. High  $T_E$  of the flows is also supported from a rock magnetic point of view by the fact that the remanences consist of single components which are very stable up to high temperatures. Examples of orthogonal plots and remanence decay curves of the thermal demagnetizations are shown in Fig. 6 for UZ14-8-2 (a) and UZ15-7-2 (b). These features in thermal demagnetization surely indicate a thermal origin of the remanences. Nevertheless, remanence directions are very scattered at UZ15 while well grouped at UZ14, as shown in the equal area plot of Fig. 7.

This puzzling fact is not so difficult to understand according to the formation model of block-and-ash flow proposed

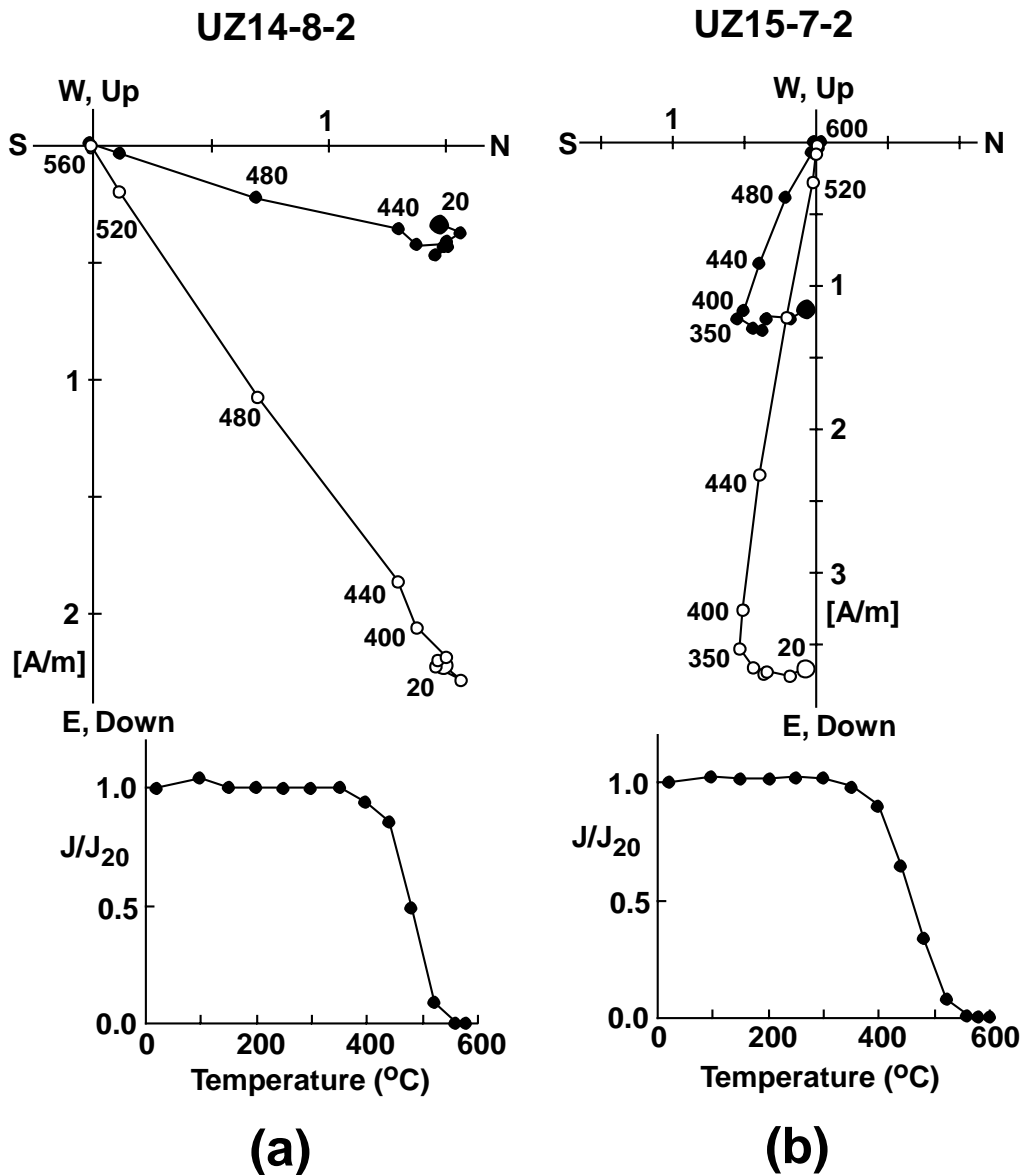


Fig. 6. Typical orthogonal plots of progressive thermal demagnetization for the Mutsugi Pyroclastic Flow (a) and the Kita-Kamikoba Pyroclastic Flow (b). Stable one-component remanence indicates a thermal origin from high temperature for both flows.

by Ui *et al.* (1999). During the stage of exogenous growth of the dome, new lava is squeezed out from the vent and slowly spreads laterally. Block-and-ash flows are generated at the frontal edge of the flow lobe. During the stage of endogenous growth, magma is intruded within the dome without the generation of lava flows on the surface. Rock falls occur when the dome is locally bulged, generating block-and-ash flows. When the lava dome is endogenously growing, the temperature of the dome wall could be lower than 300–400°C. As known from Fig. 6(b), the blocking temperature ( $T_B$ ) of the samples from UZ15 distributes between about 400°C and a Curie temperature ( $T_C$ ) of about 600°C. Hence, TRM acquisition must have been completed when the rock fall occurred, as shown in the bottom illustration in Fig. 7. During the stage of the exogenous dome, temperatures of flow lobes at the frontal edge must have been over 600°C. In this case, TRM was acquired after emplacement of the pyroclastic flow

(top figure of Fig. 7).

This idea is further supported by color observation of block samples from the two flows.  $L^*a^*b^*$  color parameters were measured by a soil color meter (MINOLTA SPAD-503). In this color system,  $L^*$  is the lightness variable, ranging 0–100%, and  $a^*$  and  $b^*$  are the chromaticity variables, where positive (negative)  $a^*$  and  $b^*$  indicate red (green) and yellow (blue), respectively (Blum, 1997). Figure 8 shows the results of color observation made of 17 and 25 pristine samples from UZ14 and UZ15, respectively. The figure includes two diagrams of  $a^*$  versus  $b^*$  (a) and  $a^*/b^*$  versus  $L^*$  (b), and closed and open circles are for UZ14 and UZ15, respectively. It is clearly seen that blocks of UZ15 are reddish while those of UZ14 are gray, indicating that blocks of UZ15 were much oxidized at the dome wall while those of UZ14 were not. Saito *et al.* (2003) made a rock magnetic study of a 2000 year-old block-and-ash flow at the Yufu Vol-

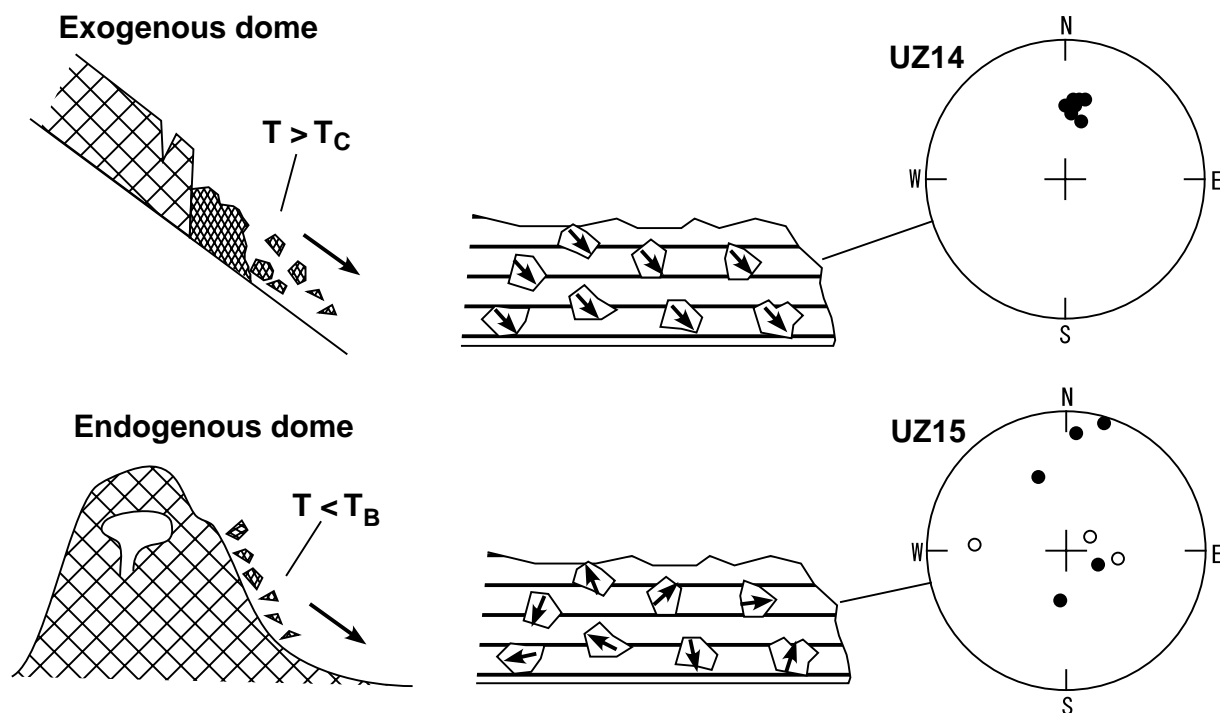


Fig. 7. Model of TRM acquisition for the two kinds of block-and-ash flows. Models of dome-forming are after Ui *et al.* (1999).

cano, Kyushu, Japan and suggested higher oxidation states for the surface samples of the lava dome than the core samples. This tendency should be enhanced when the lava dome is endogenously growing.

#### 4. Lava Identification

##### 4.1 Lavas and pyroclastic flows from ~5 ka Mayuyama Volcano

The Mayuyama Volcano is composed of northern and southern domes which are called the Shichimenzan and Tengu-yama Volcanoes, respectively. Mutsugi pyroclastic flow which distributes in the northern area of the Mayuyama Volcano, is considered to have originated from the northern dome. The purpose of the paleomagnetic study of the Mayuyama Volcano was (1) to ascertain the origin of the Mutsugi pyroclastic flow which is considered to be contemporaneous with the northern dome, and (2) to see if there is any time gap between the two domes. The simplified map in Fig. 9 shows the distribution of the domes and the pyroclastic flow, where open triangles indicate dome peaks and closed circles show site localities of the sample collection. The equal area plot in Fig. 9 shows site mean paleodirections with a circle of 95 percent confidence ( $\alpha_{95}$ ). The paleodirections from the northern dome SH (UZ05) and the pyroclastic flow (UZ14) are very close to one another with the overlapped ovals of  $\alpha_{95}$ , indicating almost the same ages for the dome and the pyroclastic flow.

On the other hand, there is significant difference between the paleodirections of the southern dome (UZ06) and those of the northern dome and the associated pyroclastic flow. Hence, it can be said that there was a time gap between the formation ages of the northern and southern domes of the

Mayuyama Volcano. The actual time difference is unknown but, with the difference angle of  $14^\circ$  between UZ05 and UZ06, it would have been several hundred years or more if a typical rate of SV for Holocene,  $2^\circ$ – $8^\circ$  per 100 years, is supposed.

Site UZ21, which was collected from the dome lava at the eastern flank of the southern dome, gave an unusual paleodirection with low inclination. This fact could indicate that this site was taken from one of the slump blocks which were formed at the 1792 collapse of the Mayuyama Volcano. One could also interpret that the paleodirection was well within normal secular variation because the corresponding virtual geomagnetic pole (VGP), which is calculated supposing an entirely dipolar paleomagnetic field, is located at  $56^\circ$ N. This is higher than the lowest VGP latitude for normal SV, which is usually taken as  $45^\circ$ . In this case, however, the lower part of the dome should be much older than the rest because no inclination as low as  $14^\circ$  was observed in the SV curves from lake sediments in Japan for the last 10 thousand years (Hyodo *et al.*, 1993; Ali *et al.*, 1999).

##### 4.2 Fukkoshi lavas of ~100 ka

Fukkoshi lava of ~100 ka is one of the lava flows that erupted from the Nodake Volcano which is the oldest volcanic center of the Younger Unzen Volcano (Tateyama *et al.*, 2002). The distribution of the lava flows is shown in the map of Fig. 10 where the open triangle is the summit of the volcano. Samples were collected at two sites from the northern flow and three sites from the eastern flow, and the site localities are shown in the map by closed circles. Corresponding site-mean paleodirections are shown in the equal area plot of Fig. 10.

The two sites from the northern flow (UZ47, UZ48) are



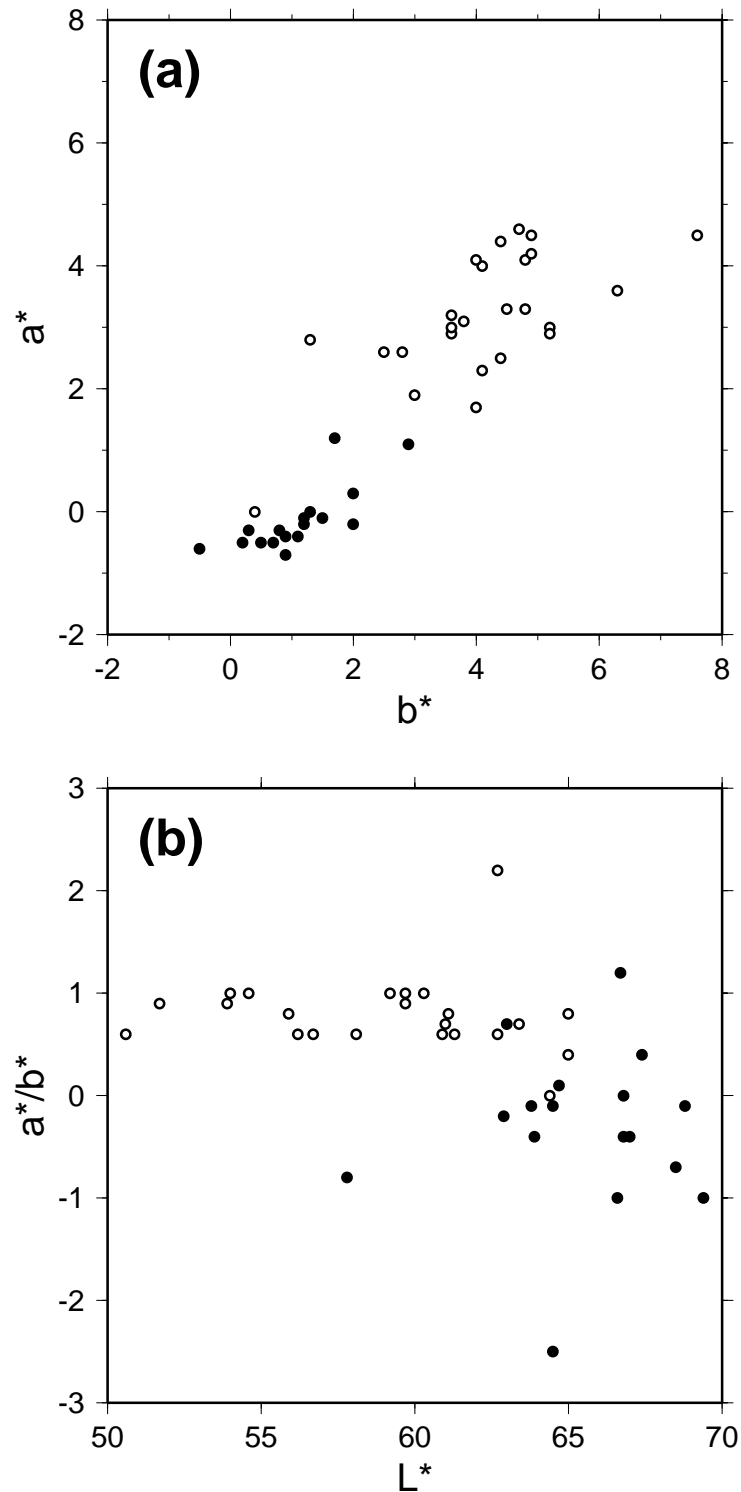


Fig. 8.  $L^*a^*b^*$  color parameters for block samples from UZ14 (closed circles) and UZ15 (open circles). Positive (negative)  $a^*$  and  $b^*$  indicate red (green) and yellow (blue), respectively (Blum, 1997). It is seen that blocks of UZ15 are reddish while those of UZ14 are gray.

only 75 m apart, but the paleodirections are not in complete agreement. Although the ovals of  $\alpha_{95}$  overlap at their edges, the statistical test of McFadden and Lowes (1981) indicates that they are significantly different. This probably illustrates a case where the paleomagnetic method does not work effectively, because these two sites are obviously from the same lava flow. Resolution of a paleodirection measured from a

certain lava flow is generally considered to be  $3\text{--}5^\circ$  (e.g., Böhm and Schnepf, 1999). The difference angle of  $4.9^\circ$  between the paleodirections from the two sites is at the same level of this resolution. This level of difference could have arisen from various error sources. The most plausible cause could be the orientation error due to a very local geomagnetic anomaly, because we could not use a sun compass at these

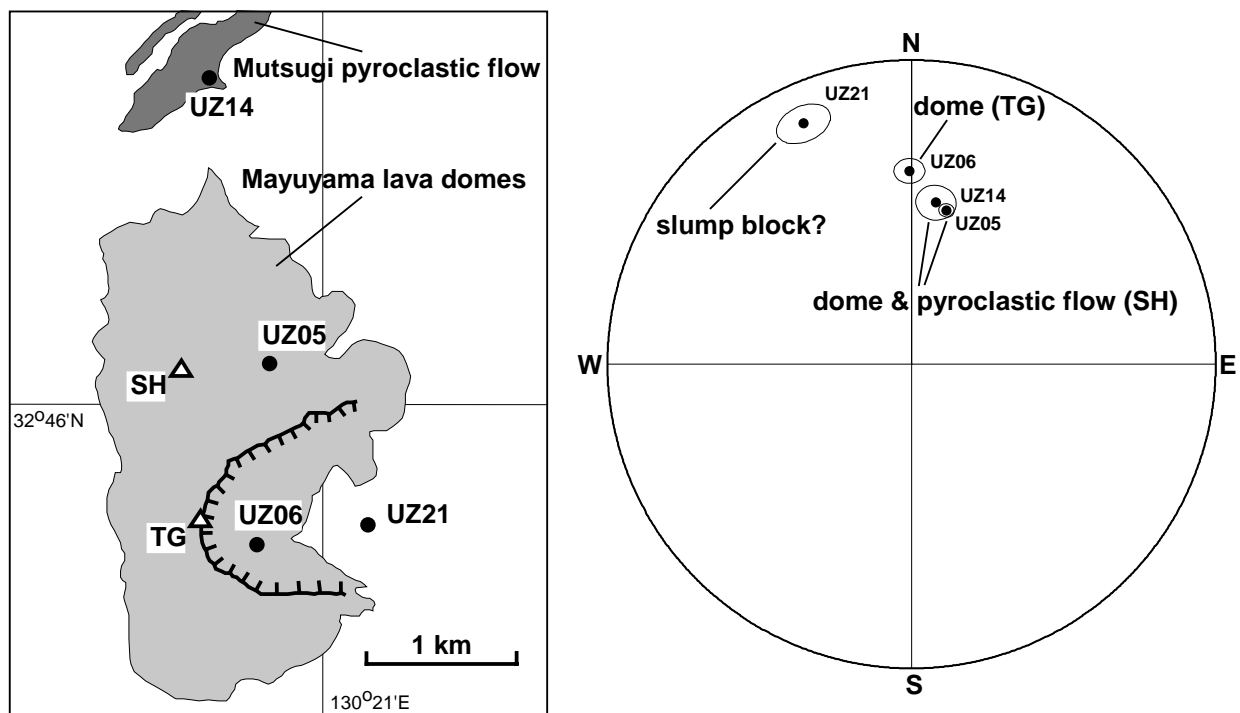


Fig. 9. Simplified map showing the distribution of lavas and pyroclastic flows originated from the Mayuyama Volcano of about 5 ka (left), and the equal area plot of remanence directions obtained from the corresponding lavas and pyroclastic flows (right). In the map, SH and TG indicate the northern (Shichimenzan) and southern (Tenguyama) domes, respectively, where an open triangle is the summit of the volcano. In the equal area plot, a closed circle and an oval around it indicate a site-mean paleodirection and 95 percent confidence circle, respectively. A possible short time lag is suggested between the northern and southern domes.

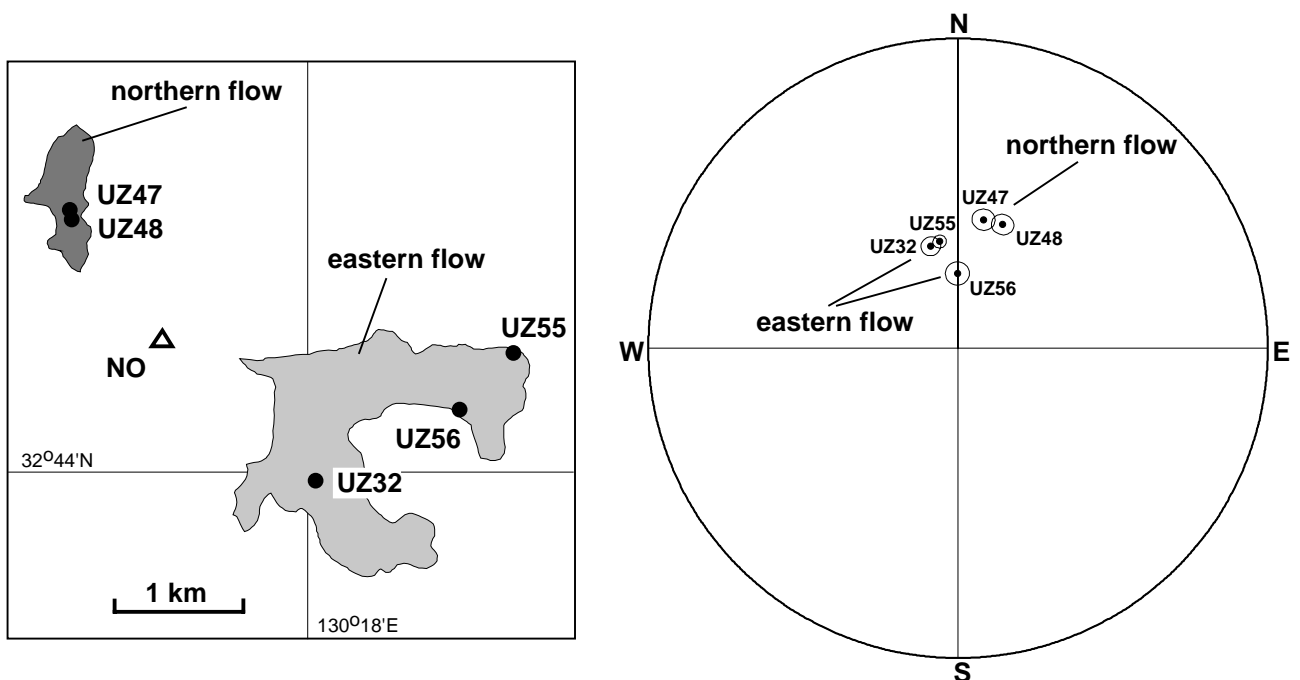


Fig. 10. Map of the northern and eastern flows of Fukkoshi lava of about 100 ka (left), and an equal area plot of site mean paleodirections (right). A possible short time lag is suggested between the northern and eastern flows, and there is a third flow which erupted at a different time. Although statistical test indicates a significant difference of the paleodirections of UZ47 and UZ48, still they are considered to represent the same lava flow because the difference angle of  $4.9^\circ$  is in the level of a resolution of the paleomagnetic method.

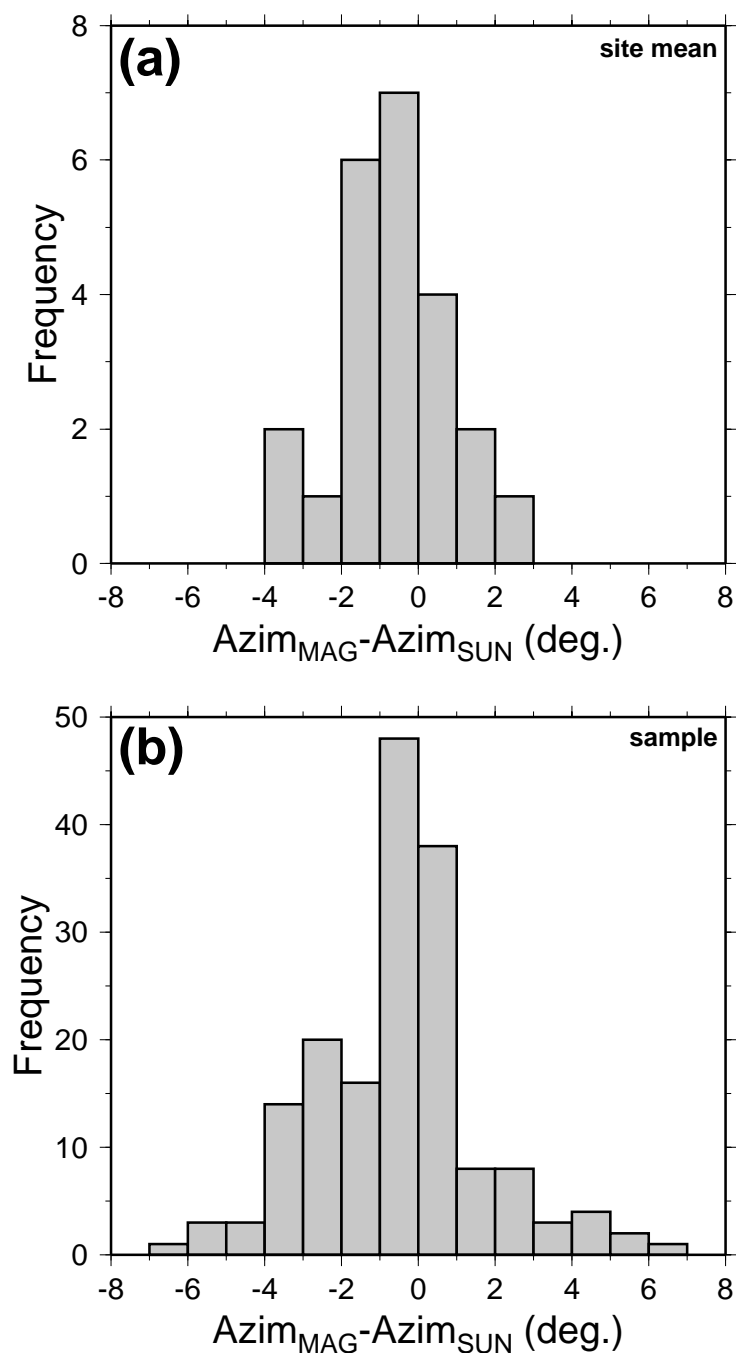


Fig. 11. Histograms of the difference angle between the sun azimuth and magnetic azimuth which were used for core orientation. Site-mean difference angles are shown in (a) and those for each core are shown in (b). It is seen that errors from the core orientation is less than  $2^\circ$  in Unzen as far as the site mean data (a) is concerned.

two sites (e.g., Castro and Brown, 1987; Baag *et al.*, 1995; Urrutia-Fucugauchi *et al.*, 2004). Small movements of the outcrop could also be the cause of the error. Nevertheless, the fact that the  $\alpha_{95}$  for each site is as small as the difference angle leads to the negative result of the statistical test of the common mean paleodirection.

Site mean paleodirections of two sites (UZ32, UZ55) from the eastern flow agree very well with a difference angle of  $2.6^\circ$  in spite of their distant locations of about 2 km. These paleodirections of the eastern flow are significantly different

from those of the northern flow, indicating that there was a certain amount of time lag, a few hundred years or more, between the eruptions of the northern and eastern flows. The problematic result is the paleodirection of one site (UZ56) from the eastern flow, which is much different from those of the other two sites from the same flow. A difference angle of more than  $10^\circ$  among paleodirections is difficult to attribute to the orientation error, even though the sun azimuth was not available at the problematic site. Hence, there could be a third flow which erupted at a different time, although the

possibility of errors caused from very large local geomagnetic anomalies or rotations of blocks cannot be ruled out.

## 5. Discussion

A wide range of  $T_E$  has been found elsewhere from different blocks within a pyroclastic flow deposit (McClelland and Druitt, 1989), although it is natural to suppose that  $T_E$  depends on a distance from the vent of eruption (Clement *et al.*, 1993). Pyroclastic deposits which contain blocks with different  $T_E$  were categorized as Type IV deposits by Hoblitt and Kellogg (1979). McClelland and Druitt (1989) interpreted such variety of  $T_E$  as that blocks of different initial temperature cooled down or heated up so that neighboring blocks came to thermal equilibrium. They also introduce an idea of average  $T_E$  of the deposit, and a general decrease of the average  $T_E$  with the distance from the vent was observed in the case of pumice fall deposits. Based on the measurements of multiple cores from the same block, Tamura *et al.* (1991) proposed an alternative interpretation that blocks of multiple component remanences indicate a cooling history of a pyroclastic flow which was initially at a uniform temperature but its highest  $T_B$  component was complicated by different rates of rolling or sliding during its transport. Our study observed one or two sharp kinks in the orthogonal plot of thermal demagnetization, as discussed in Section 3.2, and this favors the latter idea of rotations of blocks within a flow. Such complicated thermal history within a pyroclastic flow has some resemblance to the problems of aberrant remanence directions in archeological sites. Sternberg *et al.* (1999) described a case of archeological sites in Israel where anomalous directions were caused by quite a few processes including reheating and mechanical disturbances.

The error of the primary RM direction determined for a specific sample is influenced by various factors such as instrument error, orientation error, and so on. In paleomagnetism, an overall error called  $\alpha_{95}$  is used to represent such various sources of errors. The  $\alpha_{95}$  is a 95 percent confidence circle around the site-mean paleodirection. In this study, the  $\alpha_{95}$ s for site-mean paleodirections were quite small, less than  $5^\circ$ . However, a uniform bias, if contained in any of the error sources, is not represented by  $\alpha_{95}$ . A typical source of the uniform bias is an azimuth error of the sample orientation when a magnetic compass is used in the field. The azimuth error is small,  $\sim 1^\circ$ , when a sun compass is used, but the magnetic azimuth often involves much larger errors, mainly due to the local anomaly of the geomagnetic field. Fortunately in this study, the magnetic anomaly was quite small owing to relatively weak remanence of dacitic to andesitic rocks prevailing in the Unzen Volcano. Figure 11 shows histograms of difference angles between the sun and magnetic azimuths for site mean (a) and each sample (b). It is seen that the site-mean difference angle is less than  $\pm 2^\circ$  for most sites. Hence, although the sun azimuth was not available at more than half the sites in this study, we can conclude that errors caused from sample orientation at these sites are generally less than  $2^\circ$ . Nevertheless, when paleodirections are compared between different sites in which no sun azimuth is available, errors of several degrees could be included in the difference angles in extreme cases. The case of the two sites (UZ47, UZ48) from the northern flow of Fykkoshi lava

discussed in Section 4.2 might illustrate this.

## 6. Conclusions

- (1) Progressive thermal demagnetization was very effective in revealing the cooling history of non-welded pyroclastic flows. In the case of the 1991 block-and-ash flow, the primary remanences of some blocks were contaminated by very large secondary components which were thermally demagnetized only after high temperature steps of over  $500^\circ\text{C}$ . In the case of a 221 ka block-and-ash flow found at a 450 m depth of a drill core, estimated  $T_E$  varied from block to block from about 300 to over  $600^\circ\text{C}$ . Rotations of the blocks, that occurred after their settlement, were suggested for this wide range of  $T_E$  rather than a non-uniform emplacement temperature. In another case of a Holocene pyroclastic flow, remanence directions were scattered in spite of its block-and-ash flow origin. Interpretation for this contradictory observation is that probably the blocks had already cooled down below  $T_B$  at the summit when the lava dome was in the stage of endogenous formation.
- (2) Throughout the paleomagnetic measurements in this study, the precision of the remanence directions was usually less than  $5^\circ$ , as known from generally small  $\alpha_{95}$ s. The error of azimuth orientation, a typical source of a uniform bias, was quite small, less than  $\pm 2^\circ$ , even when the azimuth was magnetically determined. Nevertheless, a negative result was obtained in the common mean test which was applied to the results of the two sites from the same flow, illustrating that the resolution of paleomagnetic method is  $3\text{--}5^\circ$ , as generally considered. In spite of this limitation, in two cases of coeval lavas of Holocene and  $\sim 100$  ka, remanence directions of some of the lava flows were significantly different, indicating a time lag between the eruption of these flows.

**Acknowledgments.** This study was carried out as one of surface studies of the Unzen Scientific Drilling Project (USDP) which was financially supported by the Ministry of Education, Culture, Sports, Science, and Technology (MEXT). We thank Kozo Uto of the Geological Survey of Japan not only for his constant encouragement given to us as a project leader but also for much help in the field work. We also thank the following people for their help in the sample collection; Takeshi Saito of Kyoto University, Takako Akimasa of University of Tokyo, and Michio Furukawa of Biwa Lake Research Institute. We appreciate discussions and suggestions given by Tadahide Ui of Hokkaido University and Kazunori Watanabe of Kumamoto University. Use of a soil color meter was kindly offered by Koji Fukuma of Kumamoto University. We thank the two reviewers, Hirokuni Oda of Geological Survey of Japan and Rob Sternberg of Franklin & Marshall College, and the editor, Yasuo Ogawa of Tokyo Institute of Technology, for their constructive reviews which much improved the manuscript.

## References

- Ali, M., H. Oda, A. Hayashida, K. Takemura, and M. Torii, Holocene palaeomagnetic secular variation at Lake Biwa, central Japan, *Geophys. J. Int.*, **136**, 218–228, 1999.
- Aramaki, S. and S. Akimoto, Temperature estimation of pyroclastic deposits by natural remanent magnetism, *Am. J. Sci.*, **255**, 619–627, 1957.
- Baag, C., C. E. Helsley, S. Xu, and B. R. Lienert, Deflection of paleomagnetic directions due to magnetization of the underlying terrain, *J. Geo-*

- phys. Res.*, **100**, 10013–10027, 1995.
- Barton, C. E., D. R. Barraclough, and J. M. Quinn (eds.), Analysis and modeling of global magnetic field data and the IGRF (special volume), *J. Geomag. Geoelectr.*, **49**, 121–467, 1997.
- Blum, P., Physical properties handbook: A guide to the shipboard measurement of physical properties of deep-sea cores, Technical Note 26, Ocean Drilling Program, 1997.
- Bogue, S. W. and R. S. Coe, Paleomagnetic correlation of Columbia river basalt flows using secular variation, *J. Geophys. Res.*, **86**, 11883–11897, 1981.
- Böhm, H. and E. Schnepp, Precision of the paleomagnetic method: An example from the Quaternary Eifel volcanics (Germany), *Earth Planets Space*, **51**, 403–412, 1999.
- Castro, J. and L. Brown, Shallow paleomagnetic directions from historic lava flows, Hawaii, *Geophys. Res. Lett.*, **14**, 1203–1206, 1987.
- Clement, B. M., C. B. Connor, and G. Graper, Paleomagnetic estimate of the emplacement temperature of the long-runout Nevado de Colima volcanic debris avalanche deposit, Mexico, *Earth Planet. Sci. Lett.*, **120**, 499–510, 1993.
- Downey, W. S. and D. H. Tarling, Archaeomagnetic dating of Santorini volcanic eruptions and fired destruction levels of late Minoan civilization, *Nature*, **309**, 519–523, 1984.
- Eighmy, J. L. and R. S. Sternberg (eds.), *Archaeomagnetic Dating*, The University of Arizona Press, 446 pp, 1990.
- Enkin, R. J. and G. S. Watson, Statistical analysis of palaeomagnetic inclination data, *Geophys. J. Int.*, **126**, 495–504, 1996.
- Hagstrum, J. T. and D. E. Champion, Paleomagnetic correlation of Late Quaternary lava flows in the lower east rift zone of Kilauea Volcano, Hawaii, *J. Geophys. Res.*, **99**, 21679–21690, 1994.
- Hoblitt, R. P. and K. S. Kellogg, Emplacement temperatures of unsorted and unstratified deposits of volcanic rock debris as determined by paleomagnetic techniques, *Geol. Soc. Am. Bull.*, **90**, 633–642, 1979.
- Holcomb, R., D. Champion, and M. McWilliams, Dating recent Hawaiian lava flows using paleomagnetic secular variation, *Geol. Soc. Am. Bull.*, **97**, 829–839, 1986.
- Hoshizumi, H., K. Uto, and K. Watanabe, Geology and eruptive history of Unzen volcano, Shimabara Peninsula, Kyushu, SW Japan, *J. Volcanol. Geotherm. Res.*, **89**, 81–94, 1999.
- Hoshizumi, H., K. Uto, A. Matsumoto, S. Xu, and K. Oguri, Geology of Unzen volcano and core stratigraphy of the flank drillings, Extended abstract, Unzen Workshop 2002, Shimabara, 4–8, 2002.
- Hyodo, M., C. Itota, and K. Yaskawa, Geomagnetic secular variation reconstructed from magnetizations of wide-diameter cores of Holocene sediments in Japan, *J. Geomag. Geoelectr.*, **45**, 669–696, 1993.
- Kent, D. V., D. Ninkovich, T. Pescatore, and S. R. J. Sparks, Palaeomagnetic determination of emplacement temperature of Vesuvius AD 79 pyroclastic deposits, *Nature*, **290**, 393–396, 1981.
- Matsumoto, A., H. Hoshizumi, and K. Uto, K-Ar age determinations of USDP cores in Unzen Scientific Drilling Project and products on the surface of Unzen volcano, Extended abstract, Unzen Workshop 2002, Shimabara, 49–50, 2002.
- McClelland, E. A. and T. H. Druitt, Palaeomagnetic estimates of emplacement temperatures of pyroclastic deposits on Santorini, Greece, *Bull. Volcanol.*, **51**, 16–27, 1989.
- McFadden, P. L. and F. J. Lowes, The discrimination of mean directions drawn from Fisher distributions, *Geophys. J. R. Astr. Soc.*, **67**, 19–33, 1981.
- McIntosh, W. C., Evaluation of paleomagnetism as a correlation criterion for Mogollon-Datil ignimbrites, Southwestern New Mexico, *J. Geophys. Res.*, **96**, 13459–13483, 1991.
- Merrill, R. T., M. W. McElhinny, and P. L. McFadden, *The Magnetic Field of the Earth*, 527 pp, Academic Press, 1996.
- Miki, D., Estimate of the ages of lava flows at Sakurajima volcano, Kyushu, Japan; inferred from paleomagnetic directions and paleointensities, *Bull. Volcanol. Soc. Japan*, **44**, 111–122, 1999 (in Japanese with English abstract).
- Ozima, M., O. Oshima, and M. Funaki, Magnetic properties of pyroclastic rocks from later stage of the eruptive activity of Haruna Volcano in relation to the self-reversal of thermo-remanent magnetization, *Earth Planets Space*, **55**, 183–188, 2003.
- Saito, T., N. Ishikawa, and H. Kamata, Identification of magnetic minerals carrying NRM in pyroclastic-flow deposits, *J. Volcanol. Geotherm. Res.*, **126**, 127–142, 2003.
- Sternberg, R., E. Lass, E. Marion, K. Katari, and M. Holbrook, Anomalous archaeomagnetic directions and site formation processes at archaeological sites in Israel, *Geoarchaeology*, **14**, 415–439, 1999.
- Tamura, Y., M. Koyama, and R. S. Fiske, Paleomagnetic evidence for hot pyroclastic debris flow in the shallow submarine Shirahama Group (upper Miocene-Pliocene), Japan, *J. Geophys. Res.*, **96**, 21779–21787, 1991.
- Tanaka, H. and T. Kobayashi, Paleomagnetism of the late Quaternary Ontake Volcano, Japan: Directions, intensities, and excursions, *Earth Planets Space*, **55**, 189–202, 2003.
- Tateyama, H., H. Hoshizumi, and K. Watanabe, Stratigraphy and eruptive history of Nodake volcano, Unzen, Kyushu, Japan, *Bull. Volcanol. Soc. Japan*, **47**, 739–749, 2002 (in Japanese with English abstract).
- Ui, T., N. Matsuwo, M. Sumita, and A. Fujinawa, Generation of block and ash flows during the 1990–1995 eruption of Unzen Volcano, Japan, *J. Volcanol. Geotherm. Res.*, **89**, 123–137, 1999.
- Urrutia-Fucugauchi, J., L. M. Alva-Valdivia, A. Goguitchaichvili, M. L. Rivas, and J. Morales, Palaeomagnetic, rock-magnetic and microscopy studies of historic lava flows from the Paricutin volcano, Mexico: Implications for the deflection of palaeomagnetic directions, *Geophys. J. Int.*, **156**, 431–442, 2004.
- Uto, K., H. Hoshizumi, A. Matsumoto, and H. Nguyen, Volcanotectonic history of Shimabara Peninsula and the evolution of Unzen volcano in Southwest Japan, Extended abstract, Unzen Workshop 2002, Shimabara, 47–48, 2002.
- Verrier, V. and P. Rochette, Estimating peak currents at ground lightning impacts using remanent magnetization, *Geophys. Res. Lett.*, **29**, 1867, doi:10.1029/2002GL015207, 2002.
- Watanabe, K. and H. Hoshizumi, Geological map of Unzen volcano, Geological Map of Volcanoes 8, Geological Survey of Japan, 1995 (in Japanese with English abstract).
- Yamazaki, T., I. Kato, I. Muroi, and M. Abe, Textural analysis and flow mechanism of the Donzurubo subaqueous pyroclastic flow deposits, *Bull. Volcanol.*, **37**, 231–244, 1973.

---

H. Tanaka (e-mail: hidefumi@cc.kochi-u.ac.jp), H. Hoshizumi, Y. Iwasaki, and H. Shibuya